

Development of a Stereo Vision-based Pick and Place System for Robotic Manipulators

Thakshila THILAKANAYAKE, Nirasha HERATH, Migara LIYANAGE

(Sri Lanka Institute of Information Technology, Sri Lanka)

Abstract: Conventional robotic manipulators consist of touch and vision sensors in order to pick and place differently shaped objects. Due to the technology development and degrading sensors over a long period, the stereo vision technique has become a promising alternative. In this study, a low-cost stereo vision-based system, and a gripper to be placed at the end of the robot arm (Fanuc M10iA/12) are developed for position and orientation estimation of robotic manipulators to pick and place different shaped objects. The stereo vision system developed in this research is used to estimate the position (X, Y, Z), orientation (P_y) of the Center of Volume of four standard objects (cube, cuboid, cylinder, and sphere) whereas the robot arm with the gripper is used to mechanically pick and place the objects. The stereo vision system is placed on the movable robot arm, and it consists of two cameras to capture two 2D views of a stationary object to derive 3D depth information in 3D space. Moreover, a graphical user interface is developed to train a linear regression model, live predict the coordinates of the objects, and check the accuracy of the predicted data. The graphical user interface can also send predicted coordinates and angles to the gripper and the robot arm. The project is facilitated with python programming language modules and image processing techniques. Identification of the stationary object and estimation of its coordinates is done using image processing techniques. The final product can be identified as a device that converts conventional robot arms without an image processing vision system into a highly precise and accurate robot arm with an image processing vision system. Experimental studies are performed to test the efficiency and effectiveness of used techniques and the gripper prototype. Necessary actions are taken to minimize the errors in position and orientation estimation. In addition, as a future implementation, an embedded system will be developed with a user-friendly software interface to install the vision system into the Fanuc M10iA/12 robot arm and will upgrade the system to a device that can be implemented with any kind of customized robot arms available in the industry.

Keywords: Stereo Vision, Image Processing, Robotic Manipulators

1 Introduction

With the fast advancement of the Robotic Industry, numerous robotic applications have been created in the meantime to enhance our nature of lives drastically. One of the most significant applications that enhance our lives is the automation of robots. Robot develop-

ment is difficult for the general public as equipment and skills needed are expensive and hard to learn^[1].

This study proposes a Stereo Vision System for object identification and a custom-made gripper to place in the end effector of the Robot Arm (FANUC M10 iA/12 in order to pick and place an object. Nowadays, robots for pick and place operations are

often used in assembling and for applications like packaging, receptacle picking, and inspections mainly due to their uniformity and speed^[2].

Generally, robots for pick and place operations involve vision and touch sensors which are attached to the robot^[3]. The approach of using sensors is not productive as they degrade over time in the existence of ionizing radiation. The conventional vision method uses one camera to analyze the robot's workplace or task^[4].

Using only one camera provides a 2D image where it gives only 2D information of a scene like colors or shapes etc. 3D information of a particular scene cannot be supplied from conventional vision^[4]. Therefore, a more suitable alternative will be using a stereo vision system that uses multiple cameras for image analysis of the robot's workplace. In the stereo vision technique, two cameras will be used. Binocular cameras, in contrast to monocular vision's scale ambiguity and pure rotation issues, can directly calculate pixel depth^[5].

Stereo vision cameras will produce two stereoscopic pictures of a given scene^[6]. Thereafter the two images taken from each camera will be used for depth estimation and obtaining 3D information of the scene. The stereo vision is useful as it is an accurate and fast object coordinates identification technique. In industry, there are many robotic actuators that work using pre-defined object coordinates. Therefore, for each object, the coordinates should be preprogrammed. Hence it is an extremely time-consuming process. As a solution, this research leads to a way that can generate the position and orientation of any given standard stationary object. It is a well-known fact that using two cameras is instinctive as it models the vision system of human^[7]. At present in the manufacturing industry, most of the productions are automated, and has done many studies based on the stereo vision for production automating^[8].

The presented work uses two webcams instead of cameras with inbuilt stereo vision modules. Therefore, it leads to a cost-effective technology. At present most industrial applications can identify only a few criteria of the objects. This project suggests ways to identify

different objects using many criteria like orientation, position, shape, and color. Thus, the presented work consists of greater flexibility in the identification of stationary objects.

The end effector is a fundamental component of a robot arm that built a physical connection between the robot arm and the environment^[9]. End effectors are mostly used in many tasks including welding, pick and place, drilling, and painting. Designing a gripper at the end effector of the robot arm is task-oriented, time-consuming, and not cheaper.

This study furthermore describes the design of a mechanical gripper. The type of the gripper is categorized based on the principles used like mechanical, thermal, piezoelectrical, vacuum, electromagnetic, etc. Since 1990, various kinds of grippers have been designed and fabricated^[10].

The designed gripper is to mount on the Fanuc M10 robot arm. Usage of a well-designed gripper at the end effector of a robot arm will boost up its performance further. The gripper is actuated using a stepper motor and it can perform pick and place tasks after receiving three-dimensional coordinates and necessary dimensions of the objects. Based on those maximum and minimum parameters that the gripper should possess, a prototype was developed. The most important aspect of the designed gripper is that it can dynamically change the gripping pattern using its fingers relative to the object type. This could be done after getting the necessary dimensions, coordinates, and shape of the object.

Upon interaction with the target object, it is inevitable that some amount of force is exerted onto the object. This exerted force should be controlled precisely without damaging the object to accomplish the task successfully^[9].

Hence, in order to measure the force a calibrated Force Sensitive Resistor (FSR) is attached to one of the jaws of the gripper and is controlled using an Arduino Mega microcontroller. The FSR devices work by varying its electrical resistance and are used to measure dynamic and static forces applied on the surface of contact^[11].

The fundamental target of the presented study is to outline and assemble an installed framework, which will have the capacity to recognize an object, distinguish the 3-dimensional coordinates, recognize the position and orientation of the object. Moreover, it will have the capacity to characterize the coordinates of the object moderately with respect to the end effect of the Robot Arm.

Lastly, through the implemented framework the subtle elements of the object, for example, sort of the object, 3D Coordinates (X, Y, Z), Orientation (θ_x , θ_y , θ_z) is transmitted to the Micro-Controller of the robot arm by using a serial communication protocol.

Furthermore, in this work a new algorithm (6 Points Algorithm) to find vertices in a cube is implemented. Up to date, there are many algorithms invented by research scientists to find corner points^[12,13]. But the implemented code works successfully with a very low percentage of errors and stands out in many past invented algorithms.

2 Methodology

2.1 Design Considerations

In order to achieve the required objectives pre-processing techniques are applied as shown in Fig.1.

Throughout the study, the OpenCV module and Python Programming Language are used.

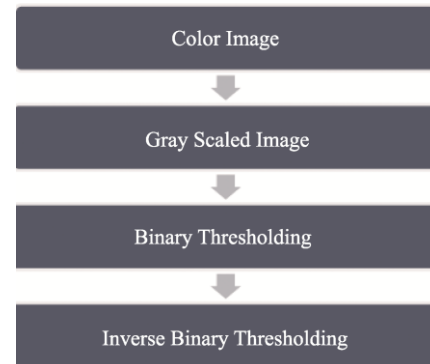


Fig.1 Preprocessing

At the end of the thresholding process, an inverted binary image of the object can be obtained as shown in the figure 2a,2b,2c,2d,2e. In this preprocessing method, the color image is firstly converted to a gray scaled image. Then converted to a binary image using the OTSU thresholding algorithm which is used for better performance. The grayscale thresholding value 100 is selected considering many influencing factors such as the light conditions and the colors of the cubes. Afterward, the binary image is inverted in order to find the contours in it.

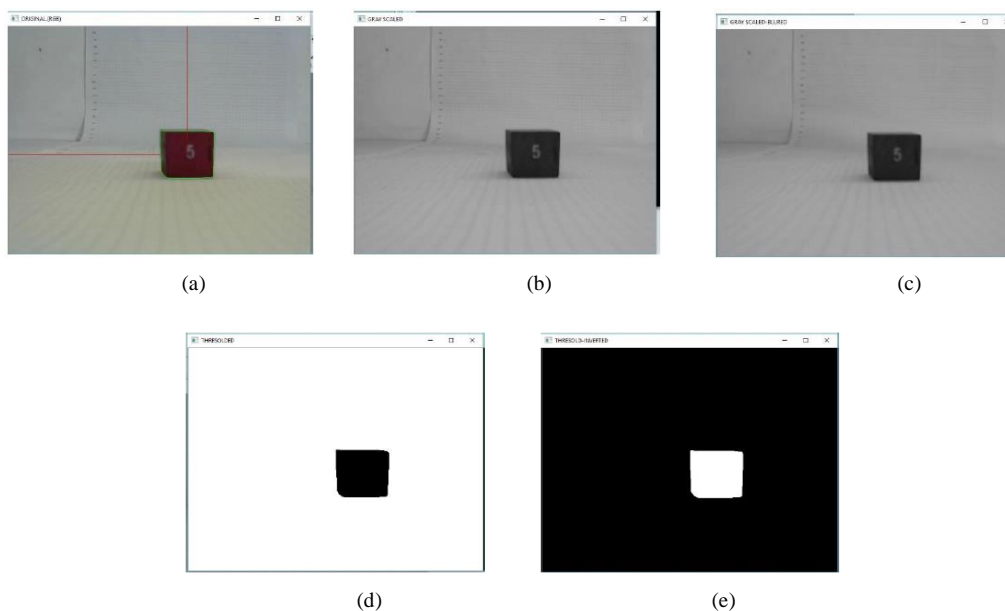


Fig.2 Binary Images (a)Color Image (b) Gray Scaled Image (c) Blurred Image (d) Binary Image (e) Invert Binary Image

In the contour detection^[14] process, there are might be contours other than the desired cube, they also will be detected. In order to overcome this situation, color filtering and contour area consideration can be done.

Since all the contours in the scene are detected, it is necessary to sort the contours and find only the required contours. In order to find the required contours following two methods were tested, 1. Sort the contour using the contour area. 2. Sort the contour using color. From the two suggested methods, it is decided to sort the contour using the color, since the robot arm is proposed to install in a white color background and the objects are in several colors. For testing, simple color ranges for Red, Green, Blue is defined and sorted the cubes according to Red, Green, and Blue as in Fig.3

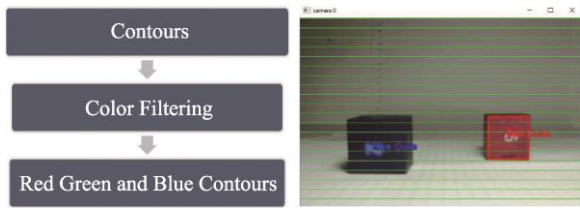


Fig.3 (a) Sorting the Contours (b) Blue and Red Cubes Sorted

Next, the shape of the object is approximated using Ramer–Douglas–Peucker algorithm^[15].The trial-and-error method was used with few samples of various sizes of cubes and spheres. The epsilon was used as $0.01 \cdot \text{Arc Length}$ of the contour. Epsilon is the maximum distance from contour to approximated contour. When the approximation is 6 it is predicted as a cube and when the approximation is greater than 6 it is predicted as a sphere.

2.2 Algorithms Used to Identify Critical Points in Different Shapes

2.2.1 6-point Algorithm for Cube and Cuboid

In this section, a newly implemented algorithm to predict the center of volume of a common cube is discussed. Although there are many algorithms invented by research scientists to find corner points^[12-13], the newly implemented algorithm shows successful results (in a 3D representation) with a very low per-

centage of errors and stands out from many past invented algorithms.

Using the Simple approximation method, the contour of the Cube is approximated. There are more than 100 boundary points in each cube contour found out. Due to the distortions and low-quality image sensor in the camera, straight lines cannot be expected in the approximated contour of the cube. To reduce the boundary points by correcting the convexity defects, the convex hull function is used. This method reduces the boundary points into a range of 30-60, using reduced convex hull points. The 6 points algorithm reduces the boundary points of the contour into 6 points as shown in Fig.4.

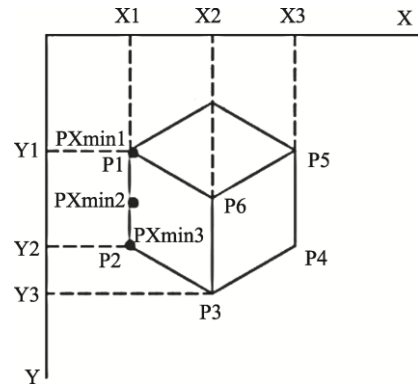


Fig.4 Six(6)-Point Algorithm with Xmin Values

As in Fig.4, the PX_{min1} , Px_{min2} , and Px_{min3} have the same X coordinate, which is $X1$, and it should be the minimum X value of the contour. In order to find the $P1$, in this case, PX_{min1} , needs to check for the points which have maximum Y value when X coordinate is X_{min} . In the same way, all other $P2$, $P3$, $P4$, and $P5$ points can be found. After collecting the coordinates for all the 5 points, the coordinates of the 6th point, $P6 = (X6, Y6)$ can be estimated.

$$X6 = X2$$

$$X6 = X2$$

$$Y6 = Y1 + (Y3 - Y2)$$

$$P6 = (X2, Y1 + (Y3 - Y2)) \quad (1)$$

This algorithm can be used to find the 6 critical points of a cube at any orientation when the cube is kept at a plane surface. When the face of the cube is

parallel to the camera lens, P3 becomes P4 and P6 becomes P5 and ultimately 4 critical points can be found. Moreover, using this algorithm all the details of the cube can be approximated. For example, the length of edge, area of the face, volume, and most importantly Center of Volume. In addition, the same algorithm with slight changes can be used to approximate the details of a cuboid. A demonstration of the 6-point algorithm is shown in Fig.5.

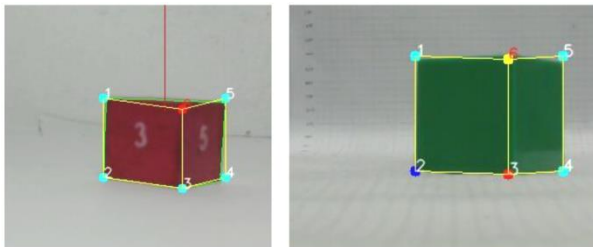


Fig.5 Demonstration of the 6-Point Algorithm

2.2.2 2-Point Algorithm for Sphere

To approximate the center of volume of a sphere, several OpenCV standard contour functions can be used. After identifying the contour as a circle using the Ramer–Douglas–Peucker algorithm, the X, Y coordinates (relative to the image plane of the camera) of the 2 critical points of a standard sphere are shown in Fig.6.

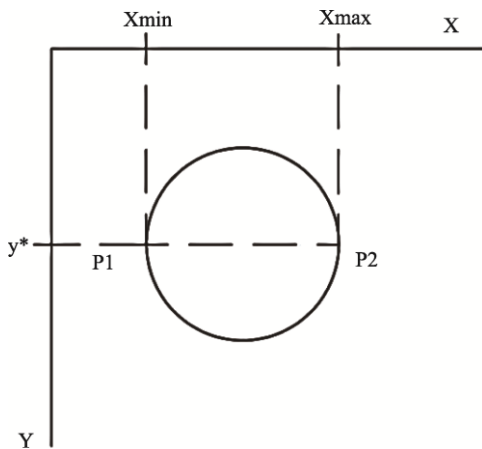


Fig.6 Two Critical Points of a Sphere

Considering the Xmin and Xmax values the coordinates of P1 and P2 can be obtained, Value of y* is the Y value of the point corresponding to Xmin or

Xmax. The Diameter of the Sphere can be approximated from $d=X_{max}-X_{min}$. In Fig.7, a demonstration of the 2 points algorithm is shown.



Fig.7 Demonstration of the 2-Point Algorithm

2.2.3 4-Point Algorithm for Cylinder

With a similar approach used for the Sphere, 4 Critical Points of a Cylinder which can be used to approximate the Center of Volume of a Cylinder can be identified as shown in Fig.8.

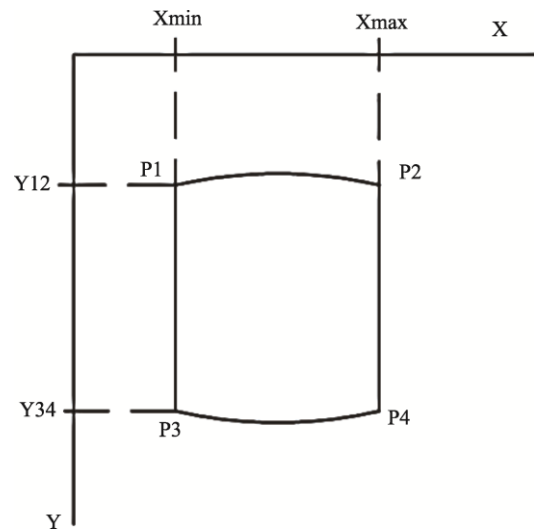


Fig.8 Four(4) Critical Points of a Cylinder

P1, P2, P3, and P4 points are approximated using Xmin, Xmax, Y12, and Y34 coordinates. In Fig.8, Y12 is found considering the minimum Y coordinate of the points, which are having X coordinate as Xmin or Xmax. Similarly, Y34 can be found considering the maximum Y coordinate of the points, which are having X coordinate as Xmin or Xmax. The height of the Cylinder can be approximated by $H=Y_{34}-Y_{12}$ and the

Diameter $D=X_{max}-X_{min}$. In Fig.9, a demonstration of the 4 points algorithm is shown.

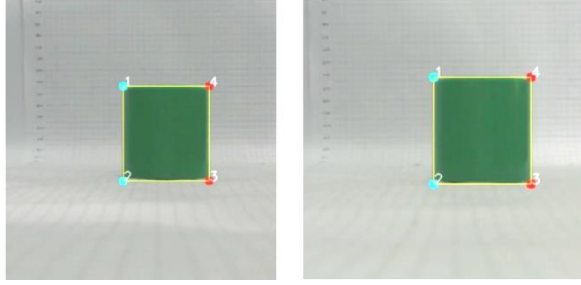


Fig.9 Demonstration of the 4-Point Algorithm

2.3 Calculating the Real World (X, Y) Coordinates of the Points in the Cube/Cuboid/Cylinder/Sphere

Using the Stereo Vision Theory and the Manual Disparity Calculation method, the real-world Z (Depth) of a pixel point as illustrated in Fig.10 is obtained with reference to the center of the image plane^[16]. To find depth information two images are taken with right and left cameras and the difference in pixel positions of the same point in two images are calculated. Depth information is found out using the triangulation method which is illustrated in Fig.10.

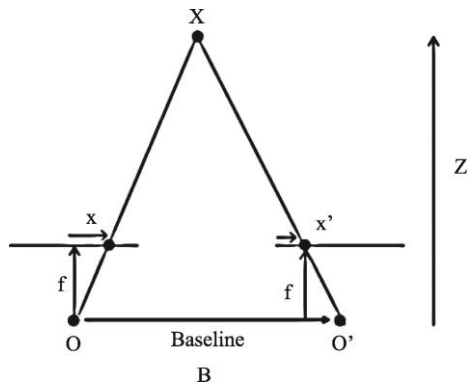


Fig.10 Triangulation Method

The depth z is

$$z = E \frac{b \cdot d}{ps} \quad (2)$$

where z is the depth to the object from the center of the camera center, B is the baseline (length between

Centers of Camera Sensors of two Cameras: 110mm in our case), ps is the pixel size of the cameras, d is the disparity of a particular point in the image and f is the focal length of a camera.

Using Equation 2, the corresponding z coordinates of all the points found from the 6-point algorithm, 2-points algorithm, and 4-points algorithms are approximated. It should be noted that this z coordinate is a predicted value. The real-world X and Y coordinates of a particular pixel point are approximated using Z (Depth) and the optimal camera matrix obtained using the camera calibration, Fig.11 shows the reverse projection of a point of the 2D image (in the camera sensor) to 3D image^[17].

Where:

X_c, Y_c, Z_c - (X, Y, Z) Axes of the camera sensor

C_x, C_y - Optical Centers of the Camera Lens

U, V - X, Y coordinates of the Image Plane

X, Y, Z - (X, Y, Z) Real World Coordinates of the Point P

By analyzing Fig.11 geometrically, equations 3 and 4^[17] are obtained to find the X, Y Real World Coordinates of P . In this situation Z (Depth) coordinate is already calculated.

$$U = f_x \frac{X}{Z} + C_x \quad (3)$$

$$V = f_y \frac{X}{Z} + C_y \quad (4)$$

For this calculation, it is assumed that the camera calibration has minimized the distortions in both cameras. C_x, C_y , and F_x, F_y can be obtained directly from the optimal camera matrix obtained from the camera calibration. It should be noted that for the Z (Depth) coordinate both the cameras should be used to take the disparity map, although, for the calculation of X, Y coordinates a single camera is used.

2.4 Approximating the Center of Volumes of Cubes, Cylinders, and Spheres

2.4.1 Approximating Center of Volume of a Cube

All the X, Y, Z coordinates of the 6 points shown in Fig.4 can be found out with respect to the camera coordinate frame. Let's assume the coordinates of the

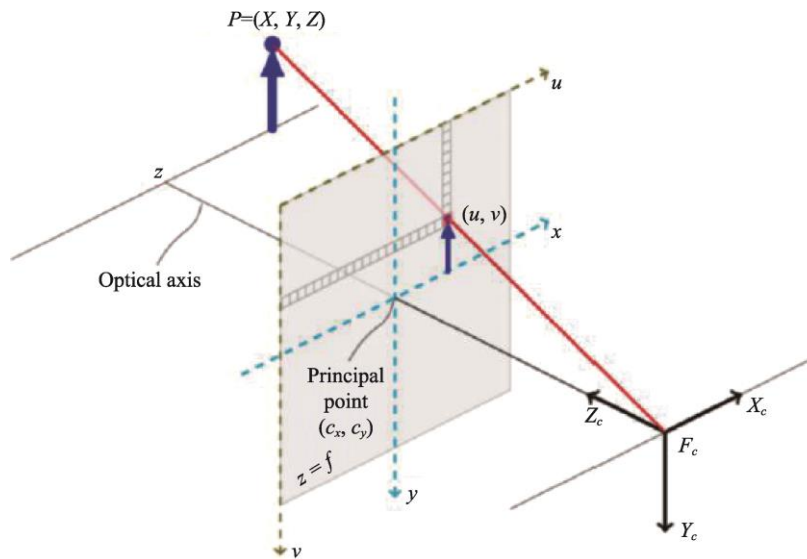


Fig.11 Reverse Projection from 2D to 3D^[17]

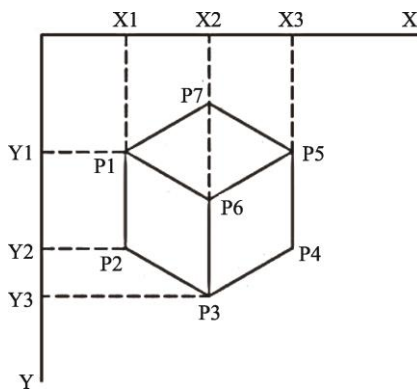


Fig.12 P7 in the Standard Cube

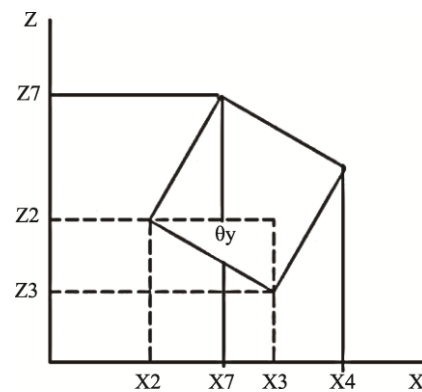


Fig.13 Plan View of Cube in Z-X Plane

center of volume of the standard cube illustrated in Fig.4 is PCV=(Xc,Yc,Zc). In order to approximate PCV, an additional point in the cube P7 is required as shown in Fig.12.

Fig.13 illustrates the plan view of the cube in the Z-X plane. The Zc and Xc can be approximated based on the Z, X coordinates of the approximated points P2, P3, P4, and P7.

The Xc, Zc, and Ycare found out using the equations 5,6, and 7 respectively. It should be noted that, instead of Y2, Y3, or Y4, Y can be used since all of them are at the same level.

$$X_c = X_2 + \frac{X_4 - X_2}{2} \tag{5}$$

$$Z_c = Z_3 + \frac{Z_7 - Z_3}{2} \tag{6}$$

$$Y_c = Y_2 + \frac{Y_2 - Y_1}{2} \tag{7}$$

2.4.2 Approximating Center of Volume of a Sphere

Assuming the coordinates of the center of volume of the standard sphere illustrated in Fig.6 is PCV=(Xc,Yc,Zc). Xc,Yc and Zc are approximated based on the real-world X,Y,Z coordinates with respect to the camera coordinate frame.

$$X_c = X_{\min} + \frac{X_{\max} - X_{\min}}{2} \tag{8}$$

$$Y_c = Y_1, Y_2 \text{ or } Y_* \tag{9}$$

$$Z_c = Z_1 \text{ or } Z_2 \tag{10}$$

2.4.3 Approximating Center of Volume of a Cylinder

Assuming the coordinates of the center of volume

of the standard cylinder illustrated in Fig.8 is PCV= (X_c, Y_c, Z_c) . X_c , Y_c and Z_c are approximated based on the real-world X,Y,Z coordinates with respect to the camera coordinate frame.

$$X_c = X_{min} + \frac{X_{max} - X_{min}}{2} \quad (11)$$

$$Y_c = Y_{34} \frac{Y_{34} - Y_{12}}{2} \quad (12)$$

$$Z_c = Z_1, Z_2 \text{ or } Z_4 \quad (13)$$

It should be noted that the P1, P2, P3, and P4 are in the same Z level. Therefore, Z_c can be approximated using a Z coordinate of any point out of those 4.

2.5 Approximating the Orientation of The Cube in Y-Axis (θ_y)

With calculated Real-World X, Y, Z coordinates of points P2, P3 the orientation of the cube in Y-axis (θ_y) in Fig.14 can findout.

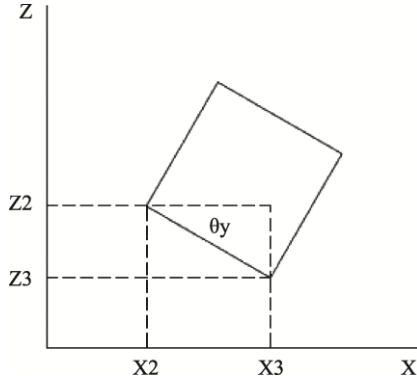


Fig.14 Orientation of the Cube: θ_y

In figure 14 the plane view (in XZ plane) of the cube is shown. The θ_y can be calculated using Equation 14.

$$\theta_y = Z_3 - Z_2 X_3 - X_2 \quad (14)$$

$P_2 = (X_2, Z_2)$ and $P_3 = (X_3, Z_3)$ of the 6 points of the cube.

2.6 Designing the Software Interface and Graphical User Interface for the Stereo Vision System

A Graphical User Interface (GUI) which has several important features is developed for the stereo

vision system. In this GUI, it has the capability to predict coordinates of the Center of the volume of standard cubes, cuboids, cylinders, and spheres. Moreover, the linear regression model can be trained using this GUI. Another important feature is that the accuracy of the predicted result can be evaluated. This software interface allows the user to send the dimensions, position, and orientation details of an object to the robot arm and the gripper. This software interface is developed using the Tkinter module available for the python programming language. Fig.15 shows the GUI designed for the stereo vision system.

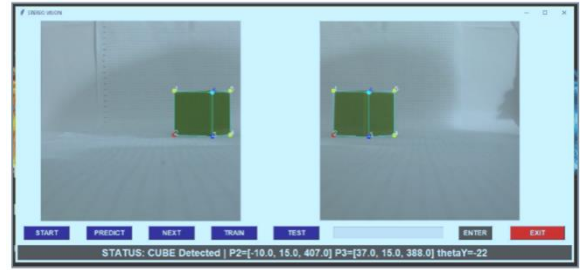


Fig.15 GUI for the Stereo Vision System

2.7 Testing the Model

To evaluate the model developed for the position and orientation estimation, a 5mmx5mm grid paper printed on A3 paper is used to place the objects. The origin of the grid paper is placed approximately at the $X=0, Z=0$ of the center of the image sensor of the right-side camera with a 15mm offset from the Y-axis of the image sensor to the origin of the XZ plane of the grid.

In the developed software interface, there are facilities for both training and testing of the stereo vision system. The linear regression model is trained using actual parameters and predicted parameters. Moreover, the linear regression model is evaluated using a known parameter and a predicted parameter,

2.8 Linear Regression to Minimize the Error

When comparing the actual and predicted data gathered, there were considerable errors, especially in Z coordinates. These errors are occurred due to many

factors such as the difference in the focal length of the left and right cameras, bad lighting conditions, low-quality camera sensors, errors in manual measurements, etc. These errors should be minimized in order to use the system in practical applications. When considering the actual and predicted parameters in almost all the situations the error has a linear behavior. Thus, it is suggested to use linear regression separately for X, Y, Z parameters of the standard cube, cylinder, and sphere objects to minimize the error.

2.9 Gripper Design

In this study, a two-jaw gripper with two small dynamically changing fingers in each jaw is designed and 3D printed to pick and place different objects. In addition to the design of the gripper, a control system is developed. An electric actuator is used for power generation and a lead screw connected to the mechanical links is used for power transmission. The structure of the gripper is made from a thermoplastic PLA (Poly Lactic Acid). A force sensor (FSR402) is used for controlling the gripping force. The force sensor is calibrated using an Arduino Mega microcontroller and weights ranging from 100g to 1000g. Arduino readings are taken by loading and unloading the weights to the force sensor.

The designed gripper can dynamically change its structure with the identification of the kind of object. Hence, the gripper can be identified as a multipurpose gripper. To achieve this feature two small links are attached to each gripper finger. The shape of the gripping surface of two small fingers is chosen according to the shape of the object. This study is to pick and place spherical, cylindrical, and cuboidal shape objects. For spherical and cylindrical shapes, the gripping surface should be in a concave shape to make object grasping efficient and for cuboidal objects, the gripping surface should be plane. In the presented design both these requirements are fulfilled as the main two fingers are in-plane shape whereas two small fingers are in a concave shape.

The presented gripper design is to mount on the end effector of the FANUC M10 iA/12 robot arm. The gripper system is a stand-alone unit with its controller

and consists of a pair of fingers, both of which are movable in opposite directions.

The gripper is controlled using Nema 17 stepper motor with an optional integrated lead screw. The gripper is designed using solid works software with a stepper motor and a lead screw. The gripper design is shown in Fig.16.

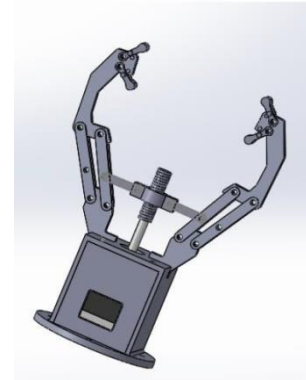


Fig.16 Gripper Design

The gripper is designed based on the requirements as in Table 1.

Table 1 Gripper Characteristics

Gripper Characteristic	Requirement
Gripping Surface	Object Shape
Gripping Range	Object Size
Gripping Force	Object Mass
Gripping Point	Object Position

3 Results and Discussion

Actual parameters and predicted parameters of critical points are recorded using the stereo vision software interface by considering 10-20 samples from each cube, cylinder, and sphere. Critical points are recorded by keeping the objects in different positions on the grid.

3.1 Actual and Predicted Coordinates of critical points in cube, cylinder, and sphere

18 samples are stored by placing the cube in different positions. Position and orientations parameters (Real World X, Y, Z) of point 2 and point 3 of 6 points

in the cube for each sample are entered with reference to image sensor using a 5mmx5mm grid and θ_y is calculated using X and Z coordinates of P2 and P3 of the 6 points. The predicted Position and Orientation parameters are taken with the implemented stereo vision and image processing methods. The actual and predicted parameters of 18 samples for P3 point are shown in Table 2. Out of 6 Critical points of a Cube, only P2 and P3 points are considered here, since P2 and P3 points are sufficient to decide the position and orientation of a standard cube. For this task 50mm length Cube is used.

In order to compare the actual and predicted parameters of the 4 critical points of a standard Cylinder, 10 samples of a cylinder that has 50mm width and 50mm height is used. For comparison between the actual and predicted value of a sphere, 10 samples of a

sphere that has a radius of 50mm are used.

It is evident that for every object in every critical point, there are considerable errors in X, Y, Z values. When analyzing the errors, a linear relationship can be identified between predicted and actual values. Using the actual and predicted values linear regression models are created for the X, Y, Z to minimize the error. Results of the linear regression models are presented in the next section.

When considering the errors of the system there can be several influencing factors like unequal focal lengths in camera lenses, lighting conditions, quality of the image sensor.

3.2 Linear Regression for Error Minimizing

In this section, the results obtained by applying the linear regression model for X, Y, Z are discussed.

Table 2 Actual and Predicted XYZ Values for P3 of a Cube

Sample No.	Predicted Coordinates of P3			Actual Coordinates of P3		
	X (mm)	Y (mm)	Z (mm)	X (mm)	Y (mm)	Z (mm)
1	69	32	575	46	15	408
2	8	29	638	2	15	472
3	38	30	503	26	15	359
4	86	27	638	60	15	479
5	26	30	582	15	15	432
6	76	29	663	58	15	489
7	28	30	586	15	15	420
8	40	30	536	26	15	387
9	26	30	551	16	15	405
10	96	27	663	70	15	511
11	66	28	654	50	15	503
12	45	27	638	35	15	495
13	18	27	616	13	15	478
14	10	29	597	8	15	454
15	28	31	569	20	15	408
16	42	31	590	31	15	419
17	46	29	515	32	15	383
18	40	30	530	27	15	385

The linear regression model is applied only for every critical point of each type of object (cubes, cylinders, and spheres). The linear regression coefficient (m) and constant (c) values of X, Y, Z, and θ_y for the cube are shown in Table 3. For this approximation 18 samples from cubes, 10 samples from cylinders, and 10 samples from spheres are used by placing the objects in different X and Y positions.

Table 3 Regression Coefficients for Cube

Parameter	Regression Coefficient (M)	Constant (mm)
X	0.7468	-4.2974
Y	0	15.0
Z	0.9630	-119.89

The graphical representation of point 2 of the cube is represented in Fig.17.

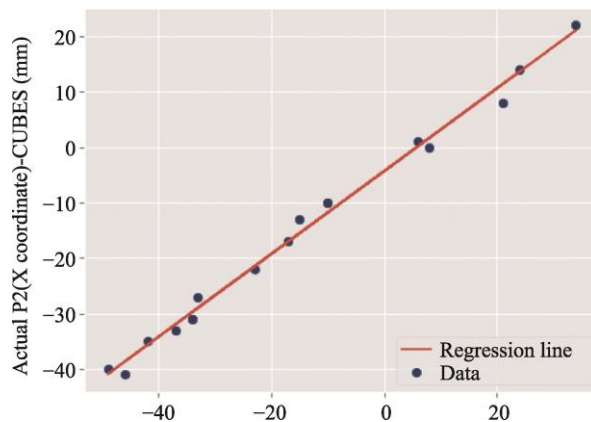


Fig.17 Regression Model for X of Point 2(Cube)

When analyzing linear regression models, it can be seen that all the models are in fine shape. To get a clear idea about the accuracy of the linear regression model implemented for the stereo vision system the R2 value is evaluated.

To test the linear regression model a sample of a cube is used by placing it in a position where P2 coordinates, P3 coordinates, and the θ_y are 10, 17, 335 (mm), 23, 17, 325 (mm) and -44.42° respectively. The

predicted values are X=9, Y=17, Z=314.46 (mm) and $\theta_y = -36.7^\circ$ as shown in Table 4. Thus, it can be concluded that the linear regression model has reduced the errors between the actual and predicted parameters up to a sufficient extent.

Table 4 Error Minimizing from Linear Regression

Parameter	Actual Value (mm)	Predicted Value Using Linear Regression Model (mm)	R2 Value
X of P2	10	9	0.9
Y of P2	17	17	1
Z of P2	335	314.46	0.94
θ_y (between P2 and P3)	-44.42	-36.7	0.84

It can be seen that all the R2 values are very close to one. (1). Thus, it is evident that the linear regression model implemented using training 38 training samples (18 Cubes, 10 Cylinders, and 10 Spheres) is an accurate model with almost 100% accuracy.

Moreover, the software interface implemented for the stereo vision system allows the user to train, enter actual position parameters and predict the position parameters of an object. As the user can add the parameters (Predicted and Actual) to the training database, the accuracy of the linear regression can be continuously improved.

3.3 Mechanical Specifications of the Gripper

The designed gripper consists of two jaws and each jaw consists of two small fingers which give the dynamically changing feature. It is evident from the specifications that, the gripper can hold very small thickness objects and objects which are having diameters, lengths, or widths less than 77mm as per the minimum and maximum distances that the gripper can retract and expand respectively. Usage of an electric actuator was beneficial as it requires low torques and is open-loop control.

The mechanical specifications of the designed gripper are shown in Table 5.

Table 5 Mechanical Specifications of the Gripper

Gripper Attributes	
Maximum Jaw Opening	77mm
Minimum Jaw Opening	0 mm
Weight Including Stepper Motor and Lead Screw	350 g
Height of the Gripper	170 mm
Material of the Prototype	PLA
Minimum Distance between Dynamic Fingers	24 mm
Finger Force	Measured Using FSR402
No. of Revolute Joint	3 in Each Jaw
No. of Prismatic Joints	0
No. of Links	3 in Each Jaw

4 Conclusions

The study was to estimate the position and orientation parameters of standard Cubic, Cylindrical and Spherical objects. The implemented algorithms work successfully with a very low percentage of errors. After implementing the linear regression models for all the types of objects, the accuracy of the models were evaluated by analyzing the R2 value. For all the coordinates, the R2 score was close to 1. Therefore, it can be concluded that the implemented linear regression models are accurate enough to use in the stereo vision system.

In this study, an electric actuator-driven gripper was designed for pick and place tasks and a prototype was 3D printed. The gripper prototype was able to dynamically change with the respect to the object's shape successfully.

As a future implementation, other error minimizing techniques will be studied and used to get more accurate results. Furthermore, an embedded system with a user-friendly software interface will be developed and installed vision system into the Fanuc M10 Robot ARM. To overcome the shortages of the work it is recommended to have good quality background light sources and to purchase a ZED stereo vision camera module for better performance in the vision System.

References

- [1] Porrill J, Pollard SB, Pridmore TP, Bowen JB, Mayhew JEW, Frisby JP. TINA: a 3D vision system for pick and place. *Image Vis Comput.* 1988; 6(2): 91-99. doi: 10.1016/0262-8856(88)90004-2
- [2] Shanta FA, Islam E, Ahammad R. Design, Construction and Performance Test of an Autonomous Low-Cost Pick and Place Robot Based on Color Detection. Published online 2020.
- [3] Kothhäuser T, Mauer GF. Vision-based autonomous robot control for pick and place operations. *IEEE/ASME Int Conf Adv Intell Mechatronics, AIM.* 2009; 24(2): 1851-1855. doi:10.1109/AIM.2009.5229792
- [4] Mohamed A, Yang C, Cangelosi A. Stereo Vision based Object Tracking Control for a Movable Robot Head. *IFAC-PapersOnLine.* 2016; 49(5): 155-162. doi: 10.1016/J.IFACOL.2016.07.106
- [5] Haige Y, Fan Y, Yanxi W. Improved Stereo Vision Robot Locating and Mapping Method. *Int J Adv Network, Monit Control.* 2019; 4(4): 47-55. doi: 10.21307/ijanmc-2019-070
- [6] Mahammed MA, Melhum AI, Kochery FA. Object Distance Measurement by Stereo VISION. *2013 Int J Sci Appl Inf Technol.* 2013; 2(2):5-8.
- [7] Sutton D, Green R. Evaluation of real time stereo vision system using web cameras. *Int Conf Image Vis Comput New Zeal.* Published online 2010. doi:10.1109/IVCNZ.2010.6148878
- [8] Bostelman R V, Albus JS, Dagalakakis NG, Jacoff A. Robocrane project : An advanced concept for large scale manufacturing. *Proc Assoc Unmanned Veh Syst Int.* Publishedonline1996. [http://www.isd.mel.nist.gov/projects/robocrane/papers.html%5CnRobocrane project - An advanced concept for large scale manufacturing.pdf](http://www.isd.mel.nist.gov/projects/robocrane/papers.html%5CnRobocrane%20project%20-%20An%20advanced%20concept%20for%20large%20scale%20manufacturing.pdf)
- [9] Kumar R, Mehta U, Chand P. A Low Cost Linear Force Feedback Control System for a Two-fingered Parallel Configuration Gripper. *Procedia Comput Sci.* 2017; 105: 264-269. doi:10.1016/J.PROCS.2017.01.220
- [10] Shaikh AH. Design and fabrication of pick and place robotic arm. *2nd Natl Conf Recent Trends Mech Eng GIST, Nellore.* 2020; (August): 16. <https://www.researchgate.net/publication/343738510%0ADesign>.
- [11] Flórez JA, Velásquez A. Calibration of force sensing resistors (fsr) for static and dynamic applications. *2010 IEEE ANDESCON Conf Proceedings, ANDESCON 2010.* Published online 2010: 2-7. doi: 10.1109/ANDESCON.2010.5633120.
- [12] Harris C, Stephens M. A Combined Corner and Edge Detector. Published online 2013: 23.1-23.6. doi: 10.5244/c.2.23
- [13] Bhujle H. An improved Harris corner detector. *ACM Int*

Conf Proceeding Ser. 2014; 14. doi: 10.1145/2683483.2683558

- [14] OpenCV: Introduction. Accessed August 23, 2021. <https://docs.opencv.org/4.5.2/d1/dfb/intro.html>
- [15] Structural Analysis and Shape Descriptors — OpenCV 2.4.13.7 documentation. Accessed August 23, 2021. https://docs.opencv.org/2.4/modules/imgproc/doc/structural_analysis_and_shape_descriptors.html?highlight=ramer+peucker
- [16] OpenCV: Depth Map from Stereo Images. Accessed August 23, 2021. https://docs.opencv.org/4.5.2/dd/d53/tutorial_py_depthmap.html
- [17] Reverse projection from 2D to 3D, I have intrinsic parameter of camera but no extrinsic parameter. I do have multiple images form same camera. - OpenCV Q&A Forum. Accessed August 23, 2021. <https://answers.opencv.org/question/171484/reverse-projection-from-2d-to-3d-i-have-intrinsic-parameter-of-camera-but-no-extrinsic-parameter-i-do-have-multiple-images-form-same-camera/>

Author Biographies



Thakshila THILAKANAYAKE. graduated from the Sri Lanka Institute of Information Technology (SLIIT) with a First-Class Honors in B.Sc. Engineering in Mechanical Engineering (Mechatronic Specialization) in 2019, and currently reading an MPhil related to Monitoring and Optimization of Domestic Energy Consumption. He is currently working as an Assistant Lecturer attached to the Department of Mechanical Engineering. His main research interest includes Robotics, Data Science, Machine Learning, and Deep Learning.

Email: thakshila.t@sliit.lk



Nirasha HERATH. graduated from the SLIIT with a First-Class Honors in B.Sc. Engineering in Mechanical Engineering (Mechatronic Specialization) in 2019. She was also awarded the merit award for academic excellence in Mechatronic Engineering from SLIIT in 2019. She is currently working as a Temporary Lecturer attached in the Department of Mechanical Engineering at Open University Sri Lanka (OUSL). She has been an Assistant lecturer at the Sri Lanka Institute of Information Technology (SLIIT).

Email: hmvhe@ou.ac.lk



Migara LIYANAGE. is serving as a Senior Lecturer attached to the Department of Mechanical Engineering at the Sri Lankan Institute of Information Technology (SLIIT). His main research interest includes Mechatronics. He is working on developing high-speed industrial automation systems for product inspection and defect removal. His work involves high-speed robotic manipulators, novel sensors, and embedded systems using Field Programmable Gate Array technology. He has authored a book and several publications in peer-reviewed journals and international conferences. He is a member of Professional Engineers and Geoscientists Newfoundland & Labrador, Canada. Dr. Migara has been a visiting lecturer at the Memorial University of Newfoundland, Canada, and Faculty of Engineering, University of Jaffna.

Email: migara.l@sliit.lk



Copyright: © 2021 by the authors. This article is licensed under a Creative Commons Attribution 4.0 International License (CC BY) license (<https://creativecommons.org/licenses/by/4.0/>).